Desalination and Water Treatment
www.deswater.com
doi: 10.1080/19443994.2014.951972

56 (2015) 1746–1757
November

Taylor & Francis
Taylor & Francis Group

Correlating ultrafiltration membrane fouling with membrane properties, water quality, and permeate flux

Haiqing Chang[a], Fangshu Qu[a], Heng Liang[a,*], Ruibao Jia[b], Huarong Yu[a], Senlin Shao[a], Kai Li[a], Wei Gao[c], Guibai Li[a]

[a]*State Key Laboratory of Urban Water Resource and Environment (SKLUWRE), Harbin Institute of Technology, No. 73 Huanghe Road, Nangang District, Harbin 150090, China, emails: changingchq@126.com (H. Chang), qufangshu@163.com (F. Qu), Tel. +86 451 86283001, Fax: +86 451 86283001; emails: hitliangheng@163.com (H. Liang), huarongyu@gmail.com (H. Yu), shaosenlin@gmail.com (S. Shao), likai02007@126.com (K. Li), hitsteven@gmail.com (G. Li)*
[b]*Jinan Water and Wastewater Monitoring Center, No. 68 Weiwu Road, Shizhong District, Jinan, 250021, China, email: jiaruibao68@126.com (R. Jia)*
[c]*The Administration Center of Urban-Rural Planning, Ministry of Housing and Urban-Rural Development of P.R. China, No. 9 Sanlihe Road, Beijing 100835, China, email: hitgaowei@163.com (W. Gao)*

Received 8 May 2014; Accepted 27 July 2014

ABSTRACT

The effect of membrane properties, feed water quality, and permeate flux on ultrafiltration (UF) membrane fouling was systematically investigated. Fouling tests were carried out with three types of commercially available UF membrane and a variety of influents. The membrane fouling was assessed by the normalized fouling rate (F_{500}). The results showed that the PVDF membrane with smaller contact angle was more resistant to membrane fouling than the PVC membrane. As for feed water parameters, significant correlations were observed between turbidity, total organic carbon, UV_{254}, fluorescence intensity, and membrane fouling rates using Pearson Correlation Analysis. This was especially true for hydraulically irreversible fouling rate (F_{irr}). Moreover, significant correlations between permeate fluxes and membrane fouling rates were observed. With these correlations, the critical flux and critical flux for irreversibility were calculated. It was found that the critical flux is strongly depended on feed water composition rather than membrane properties. Particulate matter, with a size of 0.45–1.2 μm in diameter, was proved to increase the critical flux and critical flux for irreversibility.

Keywords: Normalized fouling rate; Membrane properties; Feed water quality; Critical flux; Critical flux for irreversibility

1. Introduction

Membrane fouling remains the most severe problem and barrier to the successful application of ultrafiltration (UF) membrane for water treatment. The degree of UF membrane fouling is a complex function of membrane properties, feed characteristics, and operational condition. Thus, it is crucial to further explore the relationships of membrane fouling with these key factors.

*Corresponding author.

Briefly, membrane properties, such as pore size, surface/pore charge, hydrophobicity, and roughness, have been confirmed to exert a big impact on membrane fouling in previous literature [1–3]. In general, a hydrophobic membrane fouls to a greater extent than a hydrophilic membrane due to the hydrophobic interaction between foulants and membrane [3–5]. The streaming potential of virgin membrane influenced the initial fouling, while the fouled membrane might exhibit the electric characteristics of foulants [6,7]. Whereas, according to the results reported by Yuan and Zydney [8], a small flux decline after humic acid adsorption was observed, but the change in zeta potential was significant. Under defined hydrodynamic conditions, generally, membranes with larger pore sizes exhibited faster flux decay than that with small pore sizes [9,10].

Feed water parameters are of crucial importance for the UF membrane fouling. Citulski et al. [11] concluded that the statistical significance of turbidity on transmembrane pressure (TMP) was insignificant by statistical analysis, contrary to that for total suspended solids. By analyzing the correlations between potential foulants and UF membrane fouling of different waters, Tian et al. [12] suggested that the biopolymer content in water can be employed as a universal indicator for predicting membrane fouling potential in UF processes. According to Peldszus et al. [13], the content of protein-like substances was highly related to irreversible fouling of the UF membrane and the fouling transitions from a reversible to an irreversible regime were depended on feed composition and operating time. Whereas, Huang et al. [14] found that neither turbidity nor DOC was a universal parameter in predicting the fouling potential of feed water. Recently, liquid chromatography with organic carbon detector and fluorescence excitation emission matrices (EEM)-based principal component analysis approach or fluorescence intensity have been successfully adopted to offer a more detailed characterization of foulants [15,16]. However, the conflicting assessments are not rare, considering the effects of feed water parameters on fouling potentials. Though correlation was believed to offer more convinced information on membrane fouling and fouling indicators, a clear understanding of the statistical correlation of feed water indicators with membrane fouling rates was still lacking.

Regarding the operational condition, hydrodynamic techniques such as applied flux, relaxation, periodic backwash, air scouring have been proved to control membrane fouling. In view of the permeate flux, operation at sub-critical flux is a favorable method to control membrane fouling [17,18]. It should be noted that the critical flux had been widely reported, all with the same intention but different methods to determine it. The most widely adopted method to determine critical flux is based on short-term flux-step method [19]. Further, more and more methods have been developed: square wave barovelocimetry technique [20], improved flux-step method with relaxation [21] or pre-compression [22], long-term flux tests [23], direct observation through the membrane [24], and mass balance [25]. However, there still lacks a standard and precise protocol for identifying the critical flux, making comparison of reported data difficult. Except the discrepancies of various methods, the determined critical flux values were also suspect. Firstly, at lower fluxes, the changes of TMP limit to the reliability and sensitivity of ordinary vacuum pressure gauges or pressure sensors. Secondly, since the flux step duration prolongs, the critical issues could be encountered: the difficulties in maintaining uniform feed water condition throughout the test and the effects of fouling hysteresis during long-term operations. Moreover, the common fact is that the critical flux estimated in short-term tests cannot be used to predict long-term fouling behavior of full-scale operation [19,23,26]. Therefore, it is urgent and timely to seek for sound alternative methods to determine the critical flux. Here, a new method involving a series of filtration tests with periodic backwash for evaluating critical flux was proposed.

Therefore, the objective of the present study was to evaluate the effect of membrane properties, feed water quality, and permeate flux on UF membrane fouling.

2. Materials and methods

2.1. Feed water and water quality analysis

Two source water with and without different kinds of pretreatments were adopted in the membrane filtration tests for different purposes. One source water from a plain reservoir, located at the downstream of the Yellow River (for short YW) was selected as the feed water in order to identify fouling indicators related to fouling rates and determine the critical flux. Another source of Songhua River in Harbin (SW), Northeast of China, was employed just for the purpose of verifying the critical flux. The fundamental information of the feed water was listed in Table 1.

In the current study, the pH, turbidity, and temperature of feed water were measured using a pH meter (Mettler Toledo, Shanghai, China), a turbidimeter (Turb550, WTW, Germany), and a mercury thermometer, respectively. UV absorbance at 254 nm (UV_{254}) was determined by a spectrometer (T6, Puxi, Beijing, China). Total organic carbon (TOC) was measured by a

Table 1
Descriptions of the feed water

Water types	Descriptions
YW0	Reservoir water without any treatments
YW1	Reservoir water pre-treated with coagulation[a]—sedimentation[b]
YW2	Reservoir water pre-treated with coagulation[a]—sedimentation[b]—sand filtration[c]
SW0	River water without any treatments
SW1	River water pre-filtered through 1.2 μm mixed cellulose ester membranes
SW2	River water pre-filtered through 0.45 μm mixed cellulose ester membranes
SW3	River water pre-treated with coagulation[d]

[a]Coagulant was polyaluminum chloride (4 mg/L, calculated by Al_2O_3).
[b]The duration of sedimentation was approximately 100 min.
[c]The flow of sand filtration was 8.7 m/h.
[d]Coagulant was polyaluminum chloride (2 mg/L, calculated by Al_2O_3).

TOC analyzer (Multi N/C 2100S, Analytik Jena, Germany). Fluorescence was measured in a 1 cm cuvette using a Fluorescence Spectrophotometer (F7000, Hitachi, Japan) at excitation (Ex) wavelengths of 220–480 nm in 5 nm increments and emission (Em) wavelengths of 350–500 nm in 1 nm increments. The correction procedures detailed in previous literature [16] were used to minimize instrument and sample biases and report spectra. The contact angle measurements of the membrane fiber were carried out adopting the sessile drop technique using a contact angle goniometer (JYSP-360, Jinshengxin Testing Machine Co. Ltd, Beijing, China).

2.2. Hollow fiber UF membrane

Three kinds of commercially available hollow fiber UF membranes were employed. During the filtration of reservoir water, a polyvinyl chloride (PVC) membrane (Membrane A, Litree Co. Ltd, Suzhou, China) and a polyvinylidene fluoride (PVDF) membrane (Membrane B, Zhaojin Motian Co. Ltd, Shandong, China) were used. Regarding the river water, another PVDF membrane (Membrane C, Litree Co. Ltd, Suzhou, China) was employed. The key parameters of the membranes and the membrane modules are summarized in Table 2. A new UF membrane module was employed for each filtration test, and each module was wetted with ethanol (analytical grade) for at least 60 min prior to use.

2.3. Experimental setup and operational condition

Fig. 1 exhibits the schematic diagram of the experimental setup. The module was immersed inside a reactor (with the effective volume of 40 mL). The raw water was fed through a constant level water tank, and the effluent was drawn from the membrane module by a peristaltic pump (BT100-2 J, Longer Pump, Baoding, China). A pressure sensor (PTP708, Tuopo Electric, Foshan, China) was mounted between the membrane module and the peristaltic pump to monitor the TMP. The operation of UF membrane was controlled by a programmable logic controller, based on a time sequence of 29 min on and 1 min off in each cycle. During the stage of being off, backwash and air scouring were carried out, with a backwash flux twice the permeate flux and an aeration intensity of 18 $m^3/(m^2\,h)$ (calculated by per unit area of the membrane tank) except membrane C. The significant impact of membrane properties on membrane fouling performance was confirmed in previous tests, so a series of

Table 2
The physical characteristics of the membranes and the membrane modules

Property Membrane type	Membrane A Hollow fiber UF	Membrane B Hollow fiber UF	Membrane C Hollow fiber UF
Inner/Outer diameter (mm)	0.85/1.45	0.7/1.2	0.85/1.45
Membrane area (cm^2)	75	75	50
Nominal pore size (μm)	0.01	0.03	0.01
Flow pattern	Outside-in, submerged	Outside-in, submerged	Outside-in, submerged
Material	PVC	PVDF	PVDF

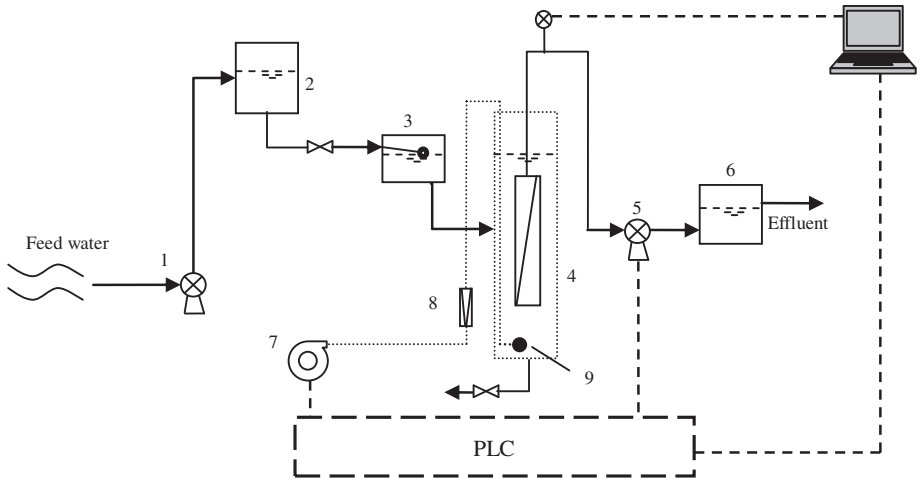

Fig. 1. Schematic diagram of the experimental setup.
Notes: (1) feed pump; (2) elevated water tank; (3) constant-level water tank; (4) UF membrane module; (5) suction (backwash) pump; (6) permeate (backwash) tank; (7) air blower; (8) air flow meter; (9) air diffuser.

Table 3
The descriptions of membrane, feed water and fluxes, and their purposes

Membrane	Feed water	Flux	Purpose
A	YW (YW0, YW1 & YW2)	9–23LMH	Fouling indicators and critical flux
B	YW (YW0, YW1 & YW2)	12–40LMH	Fouling indicators and critical flux
C	SW (SW0, SW1, SW2 & SW3)	14–73LMH	Critical flux

different fluxes were applied to different kinds of membranes. In the current study, the detailed descriptions of membrane, feed water and flux, and corresponding purposes were listed in Table 3.

2.4. Quantification of total and hydraulically irreversible fouling rates

For comparison, temperature-corrected TMPs were employed based on TMP_{20} using a temperature correction factor (TCF) according to the following equation [27]:

$$TMP_{20} = TMP_T(TCF) = TMP_T\left(\frac{\mu_{20}}{\mu_T}\right) \quad (1)$$

where μ_{20}, μ_T are the viscosities of water at 20 C and temperature T (°C), respectively, Pa·s. The viscosity of water can be approximately calculated by the following empirical equation [27]:

$$\mu_T = 1.784 - 0.0575T + 0.0011T^2 + 10^{-5}T^3 \quad (2)$$

In the present study, a normalized fouling rate index (F_{500}) was proposed to characterize the total or irreversible fouling potential of UF membranes for given feed water in multiple-cycle tests. This index was calculated by the least square linear regression approach. In this case, the final TMP (P_{tot}) and the initial TMP (P_{irr}) of each cycle represented total and hydraulically irreversible fouling, respectively. To eliminate the discrepancy of throughput per filtration time [18], the volume filtered per unit membrane area (V_s, L/m^2) instead of filtration time was employed. Therefore, the final (initial) TMP and Vs of each cycle and within the first $500\,L/m^2$ of unit permeate throughput were employed in the linear regression.

Note that the longer duration of the fouling tests, the better the membrane fouling performance could be represented, in particular, the hydraulically irreversible fouling, from the perspective of practical operation. On the other hand, considering the operation of researchers in the bench scale, the duration of each test should not be too long. In this study, a filtrate volume of $500\,L/m^2$ contains tens of cycles (according to applied flux), which could actually represent the

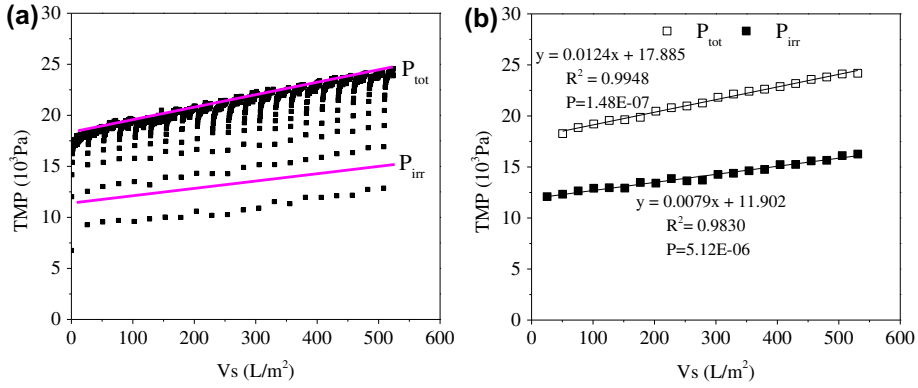

Fig. 2. An example of determining fouling rate: (a) Development of TMP in multiple-cycle filtration and (b) the calculation of F_{500} using the least square method.

fouling rates, and the drawback of short-term tests could be avoided.

An example of the calculation of F_{500} for a specific UF membrane fouling test was presented in Fig. 2. The P_{tot} and P_{irr} were determined as the average of the last or first three data points, respectively, (Fig. 2(a)) to reduce the impact of nosiy data. Then the relationships between P_{tot}, P_{irr}, and V_s were determined by the least square linear regression approach and were tested by Pearson Correlation Analysis (p-value and its correlation coefficient (R^2)). The correlation was considered statistically significant at a 95% confidence interval when p was less than 0.05 (Fig. 2(b)). Thus, the total fouling rate (F_{tot}) and the hydraulically irreversible fouling rate (F_{irr}) could be determined from the slopes of $P_{tot} - V_s$ curve and $P_{irr} - V_s$ curve, which were given by:

$$\text{Total fouling rate,} \quad F_{tot} = dP_{tot}/dV_s \tag{3}$$

$$\text{Irreversible fouling rate,} \quad F_{irr} = dP_{irr}/dV_s \tag{4}$$

Besides, compared with the qualitative observation of the fouling curves, the statistical method of cumulative probability distribution, which could provide a more comprehensive view, was used to analyze membrane fouling [14].

2.5. Critical flux based on the correlation between fouling rates and fluxes

With given feed water and membrane, the correlation between fouling rates (F_{tot}, F_{irr}) and fluxes could also be determined by the least square linear regression approach. Then the permeate flux corresponding to a null TMP increase rate can be calculated by the aforementioned correlation. It was defined as "critical flux" (J_0) for total fouling and a term "critical flux for irreversibility" (J_{0i}) was put forward in the case of hydraulically irreversible fouling. A positive x-axis intercept suggested the existence of J_0 and J_{0i}, and it is necessary to examine the feasibility of the proposed method for determining the critical flux. It should be noted that the symbols of J_0 and J_{0i} were employed instead of the commonly used J_{cr} and J_{ci} based on short-term tests (several minutes) [20–22]. Because J_0 and J_{0i} were determined by multiple-cycle filtration (with duration from several hours to days) in this study, more valuable information would be provided to the application of full-scale UF system.

3. Results and discussion

3.1. Correlation of membrane properties with membrane fouling

The total and hydraulically irreversible fouling rates for all filtration tests were summarized and listed in Tables S1 and S2 (Supporting Information). It can be observed that the F_{500} determined by the least square linear regression approach could reflect the total and hydraulically irreversible fouling rates. The linear expression between TMP and filtrate volume was also confirmed by Huang et al. [14] and Abrahamse et al. [28]. Therefore, the fouling rates were representative and could be used for further statistical analysis.

The cumulative probability distributions of F_{tot} and F_{irr} values for membrane A and B during the filtration of reservoir water were illustrated in Fig. 3. As presented in Fig. 3(a), the median values of F_{tot} for membrane A and membrane B were 16.73 and 5.66

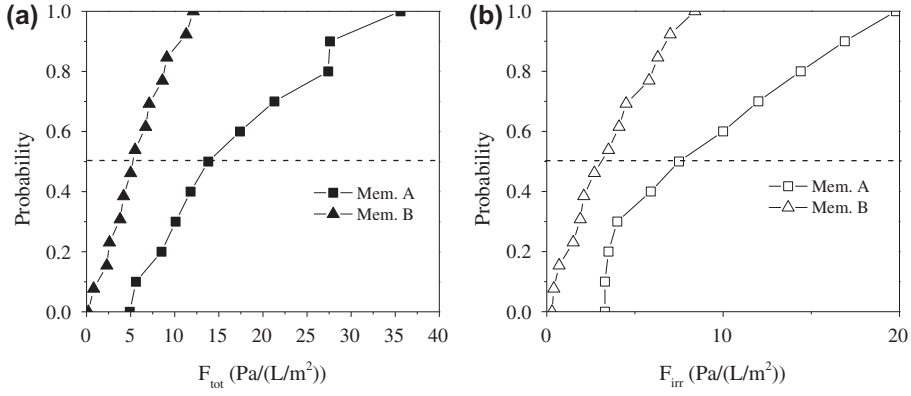

Fig. 3. Cumulative probability distributions of F_{500} with membrane properties: (a) F_{tot} and (b) $F_{irr.}$

Pa/(L/m^2), respectively. Similarly, the median value of F_{irr} for membrane A approximately tripled that of membrane B (Fig. 3(b)). It suggested a potential correlation of membrane surface and pore size with the total or hydraulically irreversible fouling rates. Moreover, the reported contact angles (the averages of eight measurements) of membrane A and membrane B were 81.2° and 60.6°, respectively. As listed in Table 2, the pore sizes of both membranes were 0.01 and 0.03 μm, respectively. It is commonly believed that the membrane with larger pore sizes fouled easily than that with small pore sizes [9,10]. Meanwhile, the importance of hydrophilicity on membrane fouling had been proved in previous reports [3]. Therefore, taking the main characteristics of both membranes into account, the role of hydrophilicity might be dominant in the current study.

3.2. Correlation of feed water quality with membrane fouling

Table 4 lists the characteristics of the main feed water quality parameters. It can be observed in Table 4 that the contents of turbidity, TOC, and UV_{254} decreased after coagulation, sedimentation or/and sand filtration. As for the fluorescence intensity, a downtrend of organic matter fractions as identified by the fluorescence EEM spectra could be found, with the result of a measurement presented in Fig. S1. Only a single peak ($\lambda_{ex/em}$ ~245/405 nm) located in Region Ⅲ was found in the raw reservoir water, indicating the main organic was fulvic acid-like substance [29]. The fluorescence intensities of the peaks in YW0, YW1, and YW2 were also listed in Table 4.

Fig. 4 presents the cumulative probability distributions of F_{tot} and F_{irr} with reservoir water. As presented in Fig. 4(a), the raw reservoir water (YW0) caused the greatest total fouling, with the median F_{tot} of 17.4 Pa/(L/m^2). The fouling potential decreased notably for the pre-treated water, making the cumulative probability distributions for YW1 and YW2 comparable. The median values of YW1 and YW2 were 8.8 and 5.3 Pa/(L/m^2), respectively, approximately half and one-third that of YW0. As exhibited in Fig. 4(b), similar results could be obtained for F_{irr}, with the median values of 10.0, 4.3, and 3.0 Pa/(L/m^2) for YW0, YW1, and YW2, respectively.

Figs. 5 and 6 exhibit the corresponding correlations of feed water turbidity, TOC, UV_{254}, and peak fluorescence intensity with the fouling rates of membrane A and membrane B, respectively. Particulate matter in water, characterized by turbidity, has already been proposed to be important membrane foulant. It can be observed in Fig. 5(a), there exist strong correlations between turbidity with both total fouling rate and irreversible fouling rate, with the R^2 values for membrane A up to 0.8243 ($p = 4.92 \times 10^{-3}$) and 0.9978 ($p = 1.14 \times 10^{-8}$), respectively. Even more significant correlations were found for membrane B, with R^2 of F_{tot} and F_{irr} above 0.999 ($p < 10^{-9}$), as shown in Fig. 6(a). This implied that turbidity might be a proper indicator of membrane fouling potential for UF of the raw water and water after coagulation, sedimentation or/and sand filtration. This observation was supported by the research of Hatt et al. [30], who identified an excellent relationship between feed water turbidity and reversible fouling in UF of the coagulated secondary effluent. The result reported by Tian et al. [12] also confirmed that turbidity could be employed as an indicator of membrane fouling potential during UF of lake water.

Regarding organic matter, the relationships between feed water organics and F_{tot} were not significant ($0.003 < p < 0.015$; $0.75 < R^2 < 0.84$) for Membrane A, as shown in Fig. 5. However, striking correlations

Table 4
Characteristics of the feed water[a]

Water types	Temperature (℃)[b]	pH[b]	Turbidity (NTU)[b]	TOC (mg L^{-1})[c]	UV_{254} (cm^{-1})[c]	Fluorescence intensity (RU)[d]
YW0	15.1 ± 2.0	8.30 ± 0.07	16.1 ± 1.1	2.45 ± 0.32	0.058 ± 0.004	0.3965
YW1	15.2 ± 1.1	8.24 ± 0.08	2.40 ± 0.80	1.29 ± 0.19	0.041 ± 0.002	0.2149
YW2	14.9 ± 1.0	8.21 ± 0.13	0.42 ± 0.03	1.09 ± 0.02	0.040 ± 0.003	0.2093
SW0	29.0 ± 0.3	7.70 ± 0.30	6.22 ± 0.32	6.49 ± 0.25	0.138 ± 0.012	na[e]
SW1	27.5 ± 0.3	8.22 ± 0.12	0.40 ± 0.08	5.68 ± 0.11	0.143 ± 0.011	na
SW2	27.5 ± 0.3	8.30 ± 0.10	0.55 ± 0.05	5.30 ± 0.12	0.134 ± 0.012	na
SW3	29.5 ± 0.3	7.98 ± 0.21	3.50 ± 0.12	5.00 ± 0.16	0.097 ± 0.015	na

[a]Values are given in average ± standard derivation.
[b]For the measurements of temperature, pH, and turbidity, the number n = 30.
[c]For TOC and UV_{254}, n = 9.
[d]Only a single peak ($\lambda_{ex/em}$ ~245/405 nm) located in Region Ⅲ was found.
[e]Without measurement.

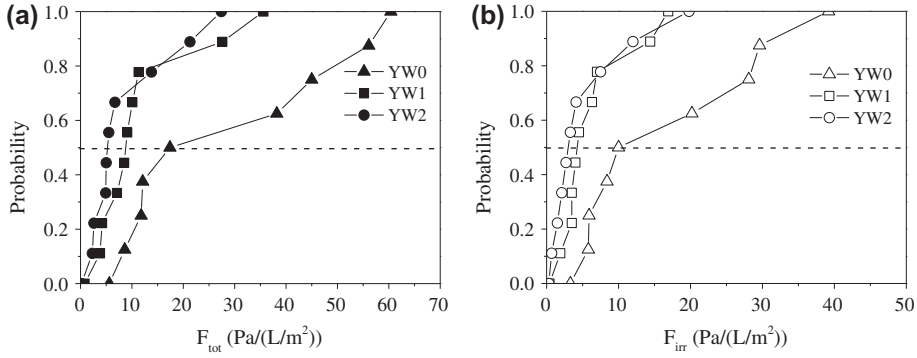

Fig. 4. Cumulative probability distributions of F_{500} with reservoir water: (a) F_{tot} and (b) F_{irr}.

were found between the organic contents and the irreversible fouling rates of membrane A, with R^2 of 0.9955 ($p = 9.83 \times 10^{-8}$), 0.9996 ($p = 6.21 \times 10^{-11}$), and 0.9981 ($p = 6.76 \times 10^{-9}$) for TOC, UV_{254}, and fluorescence intensity, respectively. On the other hand, it can be presented in Fig. 6, significant correlations were found between the organic contents and fouling rates for membrane B, regardless of the total or hydraulically irreversible one. Results reported by Henderson et al. [16] also proved the relationships between DOC, peak fluorescence intensity, and the hydraulic resistance for UF of the wastewater effluent. The finding was quite different with the results reported by Huang et al. [14], who found that the feed water DOC was only related to the fouling performance of a MF membrane rather than UF membranes.

These results indicated that feed water parameters (such as turbidity, TOC, UV_{254}, and fluorescence intensity) had potential to be used as foulant indicators in predicting the fouling rates of the raw reservoir water and treated water. This was especially the true for F_{irr}. It should be noted that three types of feed water were employed in this part, with each curve containing three points. Though few data were included, the statistical analysis migh provide meaningful implications for the relationship between membrane fouling and water quality. More feed water might be considered to verify the correlations of water parameters with membrane fouling rates for further study.

3.3. Correlation of permeate fluxes with membrane fouling

3.3.1. Correlation of fluxes with membrane fouling for UF of reservoir water

The permeate flux is strongly associated with membrane fouling. Fig. 7 elaborates both curves of the total fouling rates and hydraulically irreversible fouling rates with permeate fluxes during UF of reservoir water. Four implications can be deduced from Fig. 7 and Table 5. Firstly, gradients of curves were different for Membrane A and Membrane B, implying the

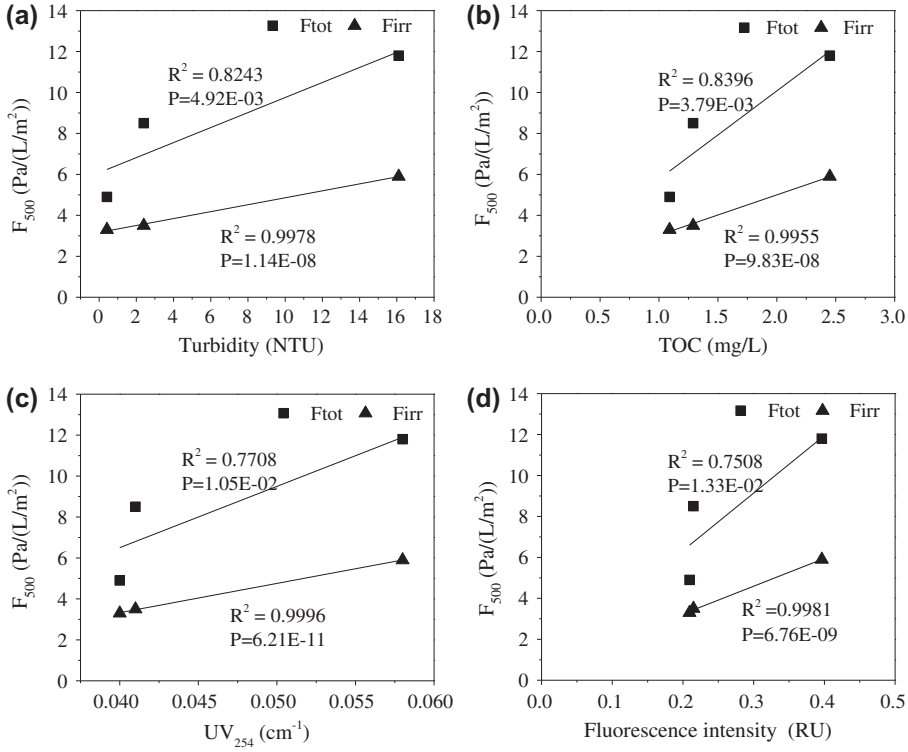

Fig. 5. Correlations of (a) turbidity, (b) TOC, (c) UV_{254}, and (d) Fluorescence intensity with membrane fouling for membrane A (average flux: 12 LMH).

discrepant fouling potentials of both membranes (Section 3.1). Secondly, gradients of lines were different for YW0, YW1, and YW2, suggesting the different fouling tendency of different feed water properties, proving the observations mentioned in Section 3.2. The third one was that strong linear relationships ($R^2 > 0.9$) between F_{tot}, F_{irr}, and fluxes were observed for most cases, proving the feasibility of the proposed method to determine critical flux statistically. The fourth one was that the positive x-axis intercepts of all the curves (F_{500} vs. fluxes) suggested the existence of J_0 and J_{0i}. The observations obtained in this research were similar with the results reported by Kwon et al. [25], who identified that a linear correlation between particle deposition rates and permeate fluxes existed. However, as reported by Le-Clech et al. [19], an exponential relationship was established between membrane fouling rates and the fluxes when the fluxes were more than 10 and 19 L/(m² h) (LMH) for real and synthetic sewage, respectively. It should be noted that surface water was employed and the maximum fluxes applied were 23 and 40 LMH for membrane A and membrane B, respectively. Therefore, F_{tot} and F_{irr} were strongly linearly related to permeate fluxes in the present study. It might indicate that the type of fouling in the present study either blocks the pores or forms a dense layer rather than pore constriction.

The values of J_0 and J_{0i} (x-axis intercepts) were also summarized in Table 5. As shown in Table 5, the values of J_0 for reservoir raw water were the smallest, and that for water after coagulation—sedimentation—sand filtration the largest, corresponding to the total fouling rates of different feed water as stated earlier (Section 3.3.1). On the other hand, there were just small differences between values of J_0 for membrane A and that of membrane B during UF of reservoir water, despite notable discrepancies were found in the total fouling rates of both membranes. Regarding the critical flux for irreversibility, similar results could be observed. Meanwhile, it can also be observed in Table 5 that the values of J_{0i} were slightly larger than that of J_0. The values of J_0 varied from 7.7 LMH to 10 LMH and J_{0i} ranged from 7.7 to 12.2 LMH, with the average values of approximately 9 and 10 LMH, respectively. The observation was consistent with the fact that J_{ci} (the critical flux for irreversibility) was larger than J_{cr} (the critical flux) in the "critical flux family" [17,21,31]. However, the values were much lower than those reported in previous literature. For instance, the J_{cr} and J_{ci} determined by Van der Marel

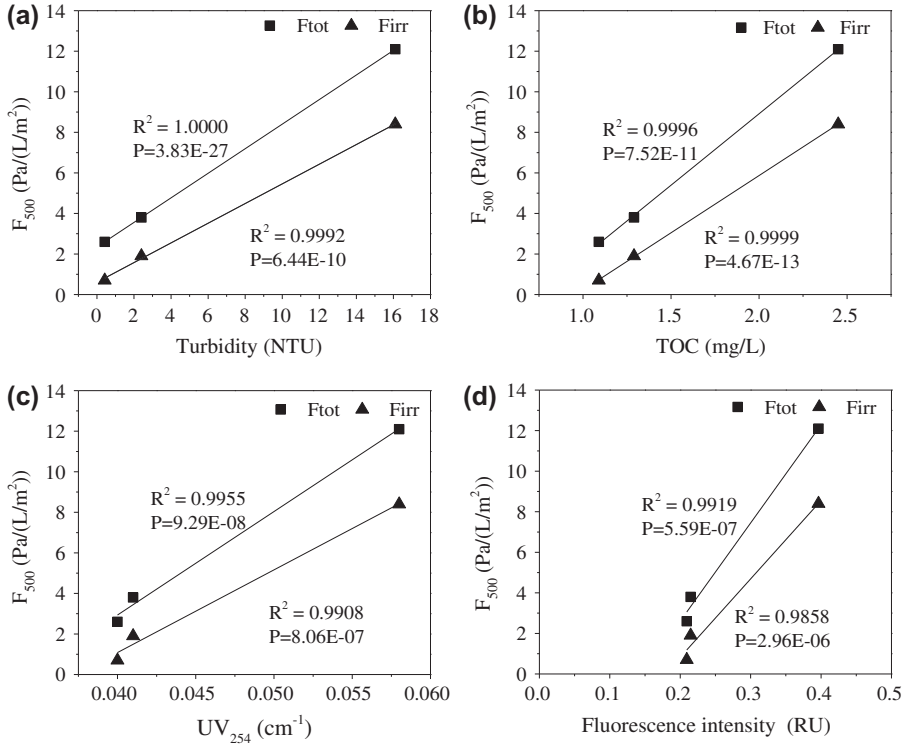

Fig. 6. Correlations of (a) turbidity, (b) TOC, (c) UV_{254}, and (d) Fluorescence intensity with membrane fouling for membrane B (average flux: 16 LMH).

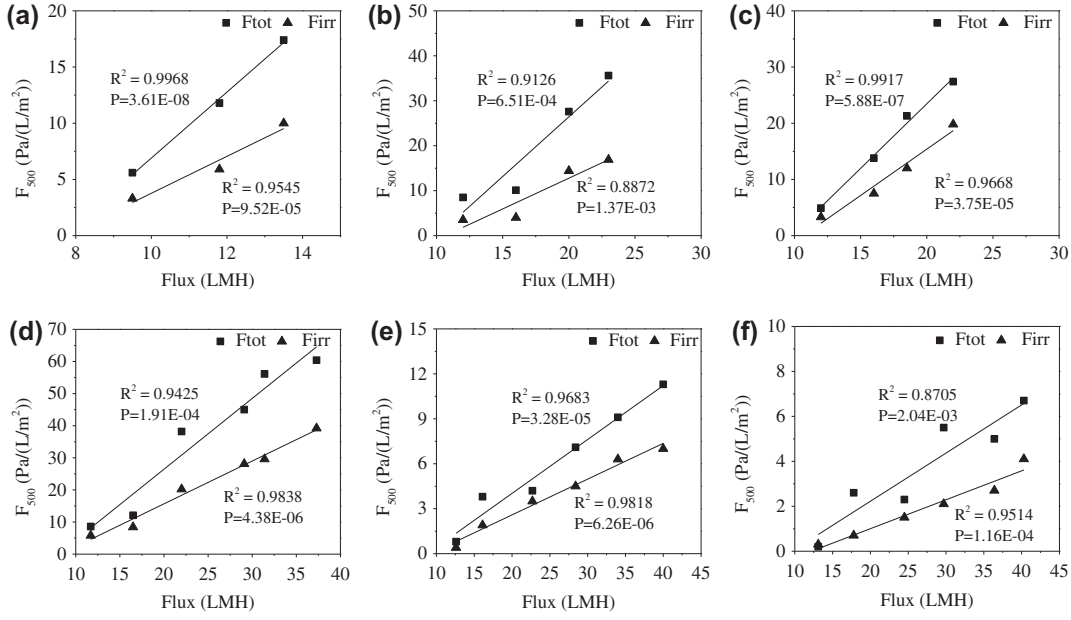

Fig. 7. Variations of membrane fouling rates with fluxes for reservoir water: (a)–(c) Membrane A and (d)–(f) Membrane B; (a) and (d) YW0, (b) and (e) YW1, and (c) and (f) YW2.

Table 5
The hydraulically irreversible fouling and total fouling characteristics of membrane A and membrane B for reservoir water

	Total fouling		Hydraulically irreversible fouling	
Membrane/water	Equation	J_0	Equation	J_{0i}
Mem.A–YW0	$y = 2.9355x - 22.452$	7.7	$y = 1.6439x - 12.669$	7.7
Mem.A–YW1	$y = 2.6538x - 26.655$	10	$y = 1.3673x - 14.569$	10.7
Mem.A–YW2	$y = 2.298x - 22.503$	9.8	$y = 1.6484x - 17.579$	10.7
Mem.B–YW0	$y = 2.2037x - 17.642$	8.0	$y = 1.332x - 10.973$	8.2
Mem.B–YW1	$y = 0.3599x - 3.1744$	8.8	$y = 0.2388x - 2.1869$	9.2
Mem.B–YW2	$y = 0.2142x - 2.0607$	9.6	$y = 0.1286x - 1.5687$	12.2

Note: y and x represent the membrane fouling rate and permeate flux, respectively.

et al. [21] in a MBR for short-term tests were 52 LMH and larger than 100 LMH, respectively. Even larger values could be expected in UF process of drinking water treatment. These results suggested that the calculated values of J_0 and J_{0i} seemed to be independent of the membrane properties but strongly related to feed water quality. This observation was coincident with the results about limiting flux reported by Tang and Leckie [6], who demonstrated that the long-term stable flux of RO/NF membrane strongly depended on feed water composition rather than membrane properties. These were probably resulted from the dominant role of foulant-deposited–foulant interaction on complete foulant coverage over membrane surfaces in long-term tests.

3.3.2. Correlation of fluxes with membrane fouling for UF of river water

To verify the feasibility of the proposed critical flux method in other source water, the procedure for determining the relationships between fluxes and membrane fouling of reservoir water were used. Fig. 8 exhibits the variations of total and hydraulically

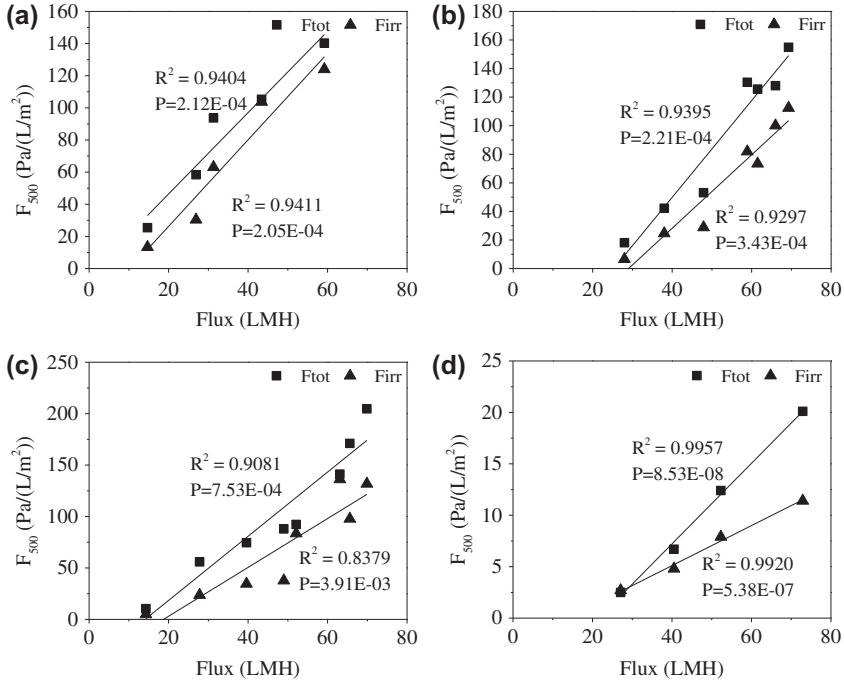

Fig. 8. Variations of membrane fouling rates with fluxes during filtration of River Water for Membrane C: (a) SW0, (b) SW1, (c) SW2, and (d) SW3.

Table 6
The hydraulically irreversible fouling and total fouling characteristics of membrane C for river water

	Total fouling		Hydraulically irreversible fouling	
Membrane/Water	Equation	J_0	Equation	J_{0i}
Mem.C–SW0	$y = 2.529x - 4.1476$	1.6	$y = 2.6916x - 27.576$	10.2
Mem.C–SW1	$y = 3.3863x - 85.61$	25.3	$y = 2.5716x - 74.667$	29.0
Mem.C–SW2	$y = 3.1184x - 43.922$	14.1	$y = 2.374x - 44.432$	18.7
Mem.C–SW3	$y = 0.3915x - 8.4464$	21.6	$y = 0.1945x - 2.6742$	13.7

Note: y and x represent the membrane fouling rate and permeate flux, respectively.

irreversible fouling rates of membrane C with fluxes, with the equations, and corresponding x-axis intercepts listed in Table 6. As presented in Fig. 8, significant linear correlations of permeate fluxes with F_{tot} and F_{irr} were observed. The smallest gradients of lines for SW3 indicated that the least fouling of SW3 amongst the four types of feed water. On the other hand, the positive x-axis intercepts of all lines suggested the existence of J_{0i} and J_0 during filtration of river water by membrane C (Table 6). As shown in Table 6, the value of J_0 for SW0 was the smallest (1.6 LMH), while that for SW1 was the largest (25.3 LMH). Compared with the raw river water, higher J_0 (21.6 LMH) was expected for coagulated water (SW3). Similar with J_0, the smallest of J_{0i} for SW0 (10.2 LMH) amongst the four feed water indicated that severe hydraulically irreversible fouling occurred during UF of the raw river water. In comparison, the J_{0i} of water after prefiltration increased significantly, with the values of 29.0 LMH and 18.7 LMH for 1.2 and 0.45 μm filters, respectively. However, compared with the raw river water, the J_{0i} for water after coagulation had not increased notably, with the values of 13.7 LMH.

As also presented in Table 6, the values of J_{0i} were larger than J_0 except for SW3, indicating that the coagulated water (SW3) could control the total fouling much more effectively than the irreversible fouling. On the other hand, the values of J_{0i} and J_0 for prefiltration with 1.2 μm filter were higher than that of 0.45 μm (by approximately 10 LMH). This observation is interesting, suggesting that the existence of a portion of particulate matter, ranging from 0.45 to 1.2 μm in diameter, could be helpful to increase the values of J_{0i} and J_0. Though just a small proportion (approximately 5%, not shown in this study) of particle size ranged between 0.45 and 1.2 μm, it influenced the membrane fouling performance.

4. Conclusions

Membrane properties had a notable impact on fouling rate and PVDF membrane with smaller contact angle exhibited a stronger resistance to membrane fouling than the PVC membrane.

The turbidity, TOC, UV_{254}, and fluorescence intensity of feed water had potential to be used as fouling indicators in predicting the membrane fouling rates, especially the hydraulically irreversible fouling rates.

Significant correlations of permeate fluxes with membrane fouling rates were observed and the values of critical flux and critical flux for irreversibility can be obtained. These values strongly depended on feed water composition rather than membrane properties. The existence of a portion of particulate matter, ranging from 0.45 to 1.2 μm in diameter, could be helpful to increase the values of J_0 and J_{0i}.

Supplementary material

The supplementary material for this paper is available online at http://dx.doi.org/10.1080/19443994.2014.951972.

Acknowledgments

This research was jointly supported by Major Science and Technology Program for Water Pollution Control and Treatment (2012ZX07404-003), Program for New Century Excellent Talents in University (NCET-13-0169), China Postdoctoral Science Foundation funded project (2013M540293), Science and Technology Planning Project of Chancheng District (2013A1044), and the Fundamental Research Funds for the Central University.

References

[1] E.M.V. Hoek, S. Bhattacharjee, M. Elimelech, Effect of membrane surface roughness on colloid-membrane DLVO interactions, Langmuir 19 (2003) 4836–4847.
[2] N. Subhi, A.R.D. Verliefde, V. Chen, P. Le-Clech, Assessment of physicochemical interactions in hollow fibre ultrafiltration membrane by contact angle analysis, J. Membr. Sci. 403–404 (2012) 32–40.

[3] H. Yamamura, K. Kimura, T. Okajima, H. Tokumoto, Y. Watanabe, Affinity of functional groups for membrane surfaces: Implications for physically irreversible fouling, Environ. Sci. Technol. 42 (2008) 5310–5315.
[4] G. Crozes, C. Anselme, J. Mallevialle, Effect of adsorption of organic matter on fouling of ultrafiltration membranes, J. Membr. Sci. 84 (1993) 61–77.
[5] H. Yamamura, K. Kimura, Y. Watanabe, Mechanism involved in the evolution of physically irreversible fouling in microfiltration and ultrafiltration membranes used for drinking water treatment, Environ. Sci. Technol. 41 (2007) 6789–6794.
[6] C.Y. Tang, J.O. Leckie, Membrane independent limiting flux for RO and NF membranes fouled by humic acid, Environ. Sci. Technol. 41 (2007) 4767–4773.
[7] C.Y. Tang, Y.N. Kwon, J.O. Leckie, Characterization of humic acid fouled reverse osmosis and nanofiltration membranes by transmission electron microscopy and streaming potential measurements, Environ. Sci. Technol. 41 (2007) 942–949.
[8] W. Yuan, A.L. Zydney, Humic acid fouling during ultrafiltration, Environ. Sci. Technol. 34 (2000) 5043–5050.
[9] A.R. Costa, M.N. de Pinho, M. Elimelech, Mechanisms of colloidal natural organic matter fouling in ultrafiltration, J. Membr. Sci. 281 (2006) 716–725.
[10] F. Qu, H. Liang, J. Zhou, J. Nan, S. Shao, J. Zhang, G. Li, Ultrafiltration membrane fouling caused by extracellular organic matter (EOM) from Microcystis aeruginosa: Effects of membrane pore size and surface hydrophobicity, J. Membr. Sci. 449 (2013) 58–66.
[11] J. Citulski, K. Farahbakhsh, F. Kent, H.D. Zhou, The impact of in-line coagulant addition on fouling potential of secondary effluent at a pilot-scale immersed ultrafiltration plant, J. Membr. Sci. 325 (2008) 311–318.
[12] J.Y. Tian, M. Ernst, F.Y. Cui, M. Jekel, Correlations of relevant membrane foulants with UF membrane fouling in different waters, Water Res. 47 (2013) 1218–1228.
[13] S. Peldszus, C. Halle, R.H. Peiris, M. Hamouda, X.H. Jin, R.L. Legge, H. Budman, C. Moresoli, P.M. Huck, Reversible and irreversible low-pressure membrane foulants in drinking water treatment: Identification by principal component analysis of fluorescence EEM and mitigation by biofiltration pretreatment, Water Res. 45 (2011) 5161–5170.
[14] H. Huang, T. Young, J.G. Jacangelo, Novel approach for the analysis of bench-scale, low pressure membrane fouling in water treatment, J. Membr. Sci. 334 (2009) 1–8.
[15] R.H. Peiris, C. Halle, H. Budman, C. Moresoli, S. Peldszus, P.M. Huck, R.L. Legge, Idendifying fouling events in a membrane-based drinking water treatment process using principal component analysis of fluorescence excitation-emission matrices, Water Res. 44 (2010) 185–194.
[16] R.K. Henderson, N. Subhi, A. Antony, S.J. Khan, K.R. Murphy, G.L. Leslie, V. Chen, R.M. Stuetz, P. Le-Clech, Evaluation of effluent organic matter fouling in ultrafiltration treatment using advanced organic characterisation techniques, J. Membr. Sci. 382 (2011) 50–59.
[17] P. Bacchin, P. Aimar, R.W. Field, Critical and sustainable fluxes: Theory, experiments and applications, J. Membr. Sci. 281 (2006) 42–69.
[18] R.W. Field, G.K. Pearce, Critical, sustainable and threshold fluxes for membrane filtration with water industry applications, Adv. Colloid Interface Sci. 164 (2011) 38–44.
[19] P. Le Clech, B. Jefferson, I.S. Chang, S.J. Judd, Critical flux determination by the flux-step method in a submerged membrane bioreactor, J. Membr. Sci. 227 (2003) 81–93.
[20] B. Espinasse, P. Bacchin, P. Aimar, Filtration method characterizing the reversibility of colloidal fouling layers at a membrane surface: Analysis through critical flux and osmotic pressure, J. Colloid Interface Sci. 320 (2008) 483–490.
[21] P. van der Marel, A. Zwijnenburg, A. Kemperman, M. Wessling, H. Temmink, W. van der Meer, An improved flux-step method to determine the critical flux and the critical flux for irreversibility in a membrane bioreactor, J. Membr. Sci. 332 (2009) 24–29.
[22] V. Diez, D. Ezquerra, J. Cabezas, A. García, C. Ramos, A modified method for evaluation of critical flux, fouling rate and *in situ* determination of resistance and compressibility in MBR under different fouling conditions, J. Membr. Sci. 453 (2013) 1–11.
[23] D. Navaratna, V. Jegatheesan, Implications of short and long term critical flux experiments for laboratory-scale MBR operations, Bioresour. Technol. 102 (2011) 5361–5369.
[24] F. Wicaksana, A.G. Fane, P. Pongpairoj, R. Field, Microfiltration of algae (Chlorella sorokiniana): Critical flux, fouling and transmission, J. Membr. Sci. 387 (2012) 83–92.
[25] D.Y. Kwon, S. Vigneswaran, A.G. Fane, R. Ben Aim, Experimental determination of critical flux in cross-flow microfiltration, Sep. Purif. Technol. 19 (2000) 169–181.
[26] A. Pollice, A. Brookes, B. Jefferson, S. Judd, Sub-critical flux fouling in membrane bioreactons—A review of recent literature, Desalination 174 (2005) 221–230.
[27] USEPA, Membrane Filtration Guidance Manual, United States Environmental Protection Agency, Office of Water, 2005.
[28] A.J. Abrahamse, C. Lipreau, S. Li, S.G.J. Heijman, Removal of divalent cations reduces fouling of ultrafiltration membranes, J. Membr. Sci. 323 (2008) 153–158.
[29] W. Chen, P. Westerhoff, J.A. Leenheer, K. Booksh, Fluorescence excitation—Emission matrix regional integration to quantify spectra for dissolved organic matter, Environ. Sci. Technol. 37 (2003) 5701–5710.
[30] J.W. Hatt, E. Germain, S.J. Judd, Precoagulation-microfiltration for wastewater reuse, Water Res. 45 (2011) 6471–6478.
[31] J. Luo, Z. Zhu, L. Ding, O. Bals, Y. Wan, M.Y. Jaffrin, E. Vorobiev, Flux behavior in clarification of chicory juice by high-shear membrane filtration: Evidence for threshold flux, J. Membr. Sci. 435 (2013) 120–129.